Molecular Therapy
Methods & Clinical Development
Original Article

Treatment with bone maturation and average lifespan of HPP model mice by AAV8-mediated neonatal gene therapy via single muscle injection

Tae Matsumoto,[1,2] Koichi Miyake,[1] Noriko Miyake,[3] Osamu Iijima,[3] Kumi Adachi,[3] Sonoko Narisawa,[4] José Luis Millán,[4] Hideo Orimo,[5] and Takashi Shimada[3]

[1]Department of Gene Therapy, Graduate School of Medicine, Nippon Medical School, 1-1-5 Sendagi, Bunkyo-ku, Tokyo 113-8602, Japan; [2]Department of Pediatrics, Nippon Medical School, 1-1-5 Sendagi, Bunkyo-ku, Tokyo 113-8603, Japan; [3]Department of Biochemistry and Molecular Biology, Nippon Medical School, 1-1-5 Sendagi, Bunkyo-ku, Tokyo 113-8602, Japan; [4]Sanford Children's Health Research Center, Sanford Burnham Prebys Medical Discovery Institute, La Jolla, CA 92037, USA; [5]Department of Metabolism and Nutrition, Graduate School of Medicine, Nippon Medical School, 1-1-5 Sendagi, Bunkyo-ku, Tokyo 113-8602, Japan

Hypophosphatasia (HPP) is an inherited skeletal disease characterized by defective bone and tooth mineralization due to a deficiency in tissue-nonspecific alkaline phosphatase (TNALP). Patients with the severe infantile form of HPP may appear normal at birth, but their prognosis is very poor. To develop a practical gene therapy for HPP, we endeavored to phenotypically correct TNALP knockout (*Akp2*$^{-/-}$) mice through adeno-associated virus type 8 (AAV8) vector-mediated, muscle-directed, TNALP expression. Following treatment of neonatal *Akp2*$^{-/-}$ mice with a single intramuscular injection of ARU-2801 (AAV8-TNALP-D10-vector) at 1.0 × 10^{12} vector genomes/body, high plasma ALP levels (19.38 ± 5.02 U/mL) were detected for up to 18 months, and computed tomography analysis showed mature bone mineralization. Histochemical staining for ALP activity in the knee joint revealed ALP activity on the surface of the endosteal bone of mice. Throughout their lives, the surviving treated *Akp2*$^{-/-}$ mice exhibited normal physical activity and a healthy appearance, whereas untreated controls died within 3 weeks. No ectopic calcification or abnormal calcium metabolism was detected in the treated mice. These findings suggest that ARU-2801-mediated neonatal intramuscular gene therapy is both safe and effective, and that this strategy could be a practical option for treatment of the severe infantile form of HPP.

INTRODUCTION

Hypophosphatasia (HPP) is an inherited systemic skeletal disease characterized by a deficiency in tissue-nonspecific alkaline phosphatase (TNALP) due to *TNALP* gene mutations, which lead to abnormal mineralization of bones and teeth.[1–3] Patients with the infantile form may appear normal at birth, but they gradually develop rickets as a clinical symptom within 6 months of age. Subsequent craniosynostosis and nephrocalcinosis follow hypercalcemia and hypercalciuria in many cases.[4] In addition, pyridoxine-dependent seizures preceding skeletal change are a predictor of lethal outcome.[5] Skeletal changes leading to thoracic deformity and rib fracture cause respiratory problems, which sometimes threaten the lives of these patients.

In adult HPP patients, some benefit has been derived from several treatment approaches, including enzyme replacement therapy (ERT) to increase plasma ALP levels[6–8] and administration of parathyroid hormone.[9,10] However, there are some problems about ERT for HPP patients, such as the emergence of antibodies for the recombinant enzyme (which may be exacerbated by chronic exogenous dosing) and difficulty transferring the enzyme to the central nervous system. Improvement of infantile HPP patients has reportedly been achieved through bone marrow transplantation.[11,12] Allogenic mesenchymal stem cell transplantation was proven for perinatal lethal HPP apothanasia and bone mineralization for 3 years, although cell therapy is always accompanied with chemotherapy, radiation therapy, and immunotherapy before the therapy and possible graft-versus-host disease after transplantation, which threaten patients' lives.[13] Even better results were observed in mice administered recombinant TNALP fused with deca-aspartate (D10) to target bone.[14] Those results led to the development of an ERT with TNALP-D10 for human HPP patients.[15] This important breakthrough improved survival times for patients with severe infantile HPP as well as the quality of life of both children and adults with HPP. However, ERT requires frequent subcutaneous injections (up to six times per week), which is burdensome for patients in terms of time, pain, and costs. The most frequent adverse effect of ERT is injection site reactions related to the frequency of the subcutaneous injections.[16]

Gene therapy has proved to be a useful tool for the treatment of several inherited diseases. In an earlier study, we succeeded in treating TNALP knockout (*Akp2*$^{-/-}$) mice, a rodent model of HPP, with a single intravenous injection of a lentiviral or adeno-associated virus

Received 2 February 2020; accepted 4 June 2021;
https://doi.org/10.1016/j.omtm.2021.06.006.

Correspondence: Koichi Miyake, MD, PhD, Department of Gene Therapy, Graduate School of Medicine, Nippon Medical School, 1-1-5 Sendagi, Bunkyo-ku, Tokyo 113-8602, Japan.
E-mail: kmiyake@nms.ac.jp

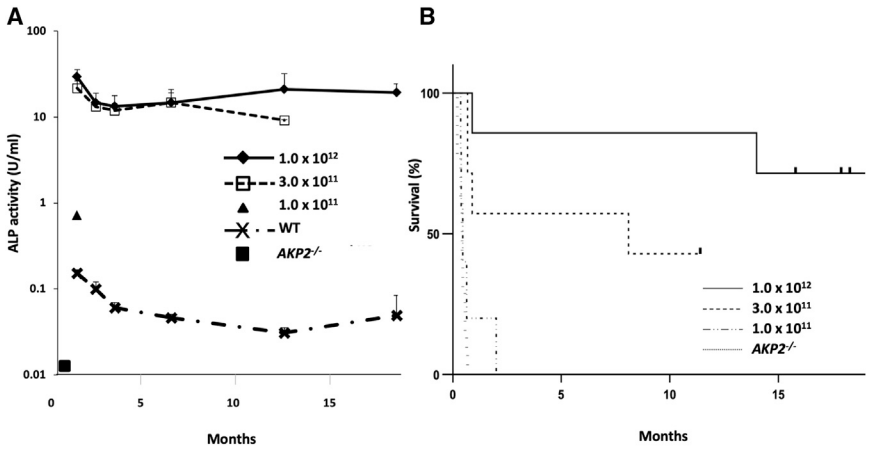

Figure 1. Plasma alkaline phosphatase (ALP) concentration and the lifespan of ARU-2801-vector (AAV8-TNALP-D10)-treated *Akp2*$^{-/-}$ mice

(A) ARU-2801 (1.0×10^{11}, 3.0×10^{11}, or 1.0×10^{12} vg/body) was injected into the right quadriceps of neonatal *Akp2*$^{-/-}$ mice. ALP activity was determined up to 18 months. (B) The lifespan up to 18 months is shown. The numbers in each mouse group were as follows: 1.0×10^{11}, n = 5; 3.0×10^{11}, n = 7; 1.0×10^{12}, n = 7; wild-type (WT), n = 5; non-treated *Akp2*$^{-/-}$ mice, n = 4.

type 8 (AAV8) vector encoding TNALP-D10, which led to sustained expression of TNALP and phenotypic correction of *Akp2*$^{-/-}$ mice.[14,17] However, intravenous injection of AAV vector leads to distribution of the vector to the whole body, which could potentially cause cancer or transduction into germ cells. Intramuscular injection may limit the vector's distribution. We therefore treated *Akp2*$^{-/-}$ mice through intramuscular injection of a vector encoding *TNALP* with a muscle-specific creatine kinase (MCK) promotor and achieved prolonged survival of *Akp2*$^{-/-}$ mice.[18,19] However, the muscle-specific expression was not sufficient to mediate bone maturation in *Akp2*$^{-/-}$ mice comparable to that in *Akp*$^{+/+}$ wild-type (WT) mice. In the present study, therefore, to develop a practical and safe gene therapy for HPP, we ventured to inject ARU-2801, an AAV8-TNALP-D10-vector with a non-tissue-specific constitutive promotor, into the right quadriceps femoris muscle and evaluated the beneficial and adverse effects in *Akp2*$^{-/-}$ mice over a prolonged period of time.

RESULTS

Survival and sustained TNALP expression in mice intramuscularly injected with more than 3.0×10^{11} vector genomes (vg)/body ARU-2801

From our previous intravenous treatment studies,[17,20] we expected that the exogenous plasma ALP activity needed for survival of *Akp2*$^{-/-}$ mice would be around 10 U/mL, which is 100-fold higher than the endogenous activity in WT mice. To determine the amount of vector needed to achieve a titer able to support *Akp2*$^{-/-}$ mouse survival, neonatal mice were first intramuscularly injected with ARU-2801 (1.0×10^{12} vg/body). The mice were then monitored to determine whether TNALP delivery via intramuscular ARU-2801 injection could phenotypically correct *Akp2*$^{-/-}$ mice. For 2 months after ARU-2801 injection, plasma ALP activity in the treated mice remained markedly higher than in WT mice (14.8 ± 4.3 versus 0.1 ± 0.004 U/mL at 2 months) (Figure 1A). Moreover, five of the seven treated mice survived for more than 18 months (Figure 1B), and sustained expression of ALP activity was confirmed, even at 18 months (19.38 ± 5.02 U/mL) (Figure 1A). Treatment failed in two mice; one died on day 25 and the second died on day 393. In similar fashion, we also tested the efficacy of administering lower doses of 3.0×10^{11} or 1.0×10^{11} vg/body ARU-2801 to determine the lowest vector strength needed for phenotypic correction of these mice. *Akp2*$^{-/-}$ mice treated with 3.0×10^{11} vg/body also showed strong ALP activity (Figure 1A) and lived for more than 12 months until sacrifice (n = 3/7 survived) (Figure 1B). In contrast, with one exception, mice administered 1.0×10^{11} vg/body died within 3 weeks (n = 1/5 survived), and in the remaining mouse, ALP activity reached 0.7 U/mL at 2 months, and the mouse died soon thereafter.

This prolonged survival showed that at vector doses of 3.0×10^{11} vg/body or higher, plasma ALP activity reaches a plateau sufficient to sustain the treated mice throughout their life. We did not find any convulsion in these treated *Akp2*$^{-/-}$ mice. We did not observe the expected dose dependency of plasma ALP activity. Although 3.0×10^{11} vg/body ARU-2801 showed significant effects, 1.0×10^{12} vg/body ARU-2801-treated mice were further analyzed given their higher survival rate.

Mature bone mineralization in mice treated with 1.0×10^{12} vg/body ARU-2801 *Akp2*$^{-/-}$ at 18 months

Sustained ALP activity not only prolonged the lives of *Akp2*$^{-/-}$ mice, it also improved the maturity of their bone mineralization. There was no significant difference in average body weight between WT mice (n = 3) and 1.0×10^{12} vg/body ARU-2801-treated *Akp2*$^{-/-}$ (n = 5) mice (Figures 2A and 2B). Secondary ossification centers were detected in all of the WT mice (n = 8/8) 10 days after birth. Alternatively, most of the untreated *Akp2*$^{-/-}$ mice did not have secondary ossification centers on day 10 (n = 3/10) (Figure 2C). After treatment, secondary ossification centers were found on day 10 in 1.0×10^{12} vg/body ARU-2801-treated *Akp2*$^{-/-}$ mice (n = 9/10) similar to those seen in WT mice. When grown to adults, on day 56, X-ray analysis of the knee joint showed mature bone in 1.0×10^{12} vg/body ARU-2801-treated *Akp2*$^{-/-}$ mice, the same as found in WT mice (Figure 2D). Untreated *Akp2*$^{-/-}$ mice, however, did not survive to adulthood (no survival by day 21) and were therefore not possible to analyze.

We next used computed tomography (CT) to analyze the structure of the femurs of 18-month-old 1.0×10^{12} vg/body ARU-2801-treated *Akp2*$^{-/-}$ mice (n = 4) and AAV8-GFP-vector-treated WT mice as control (n = 3). At 18 months, bone mineral densities (673.7 ± 41.6

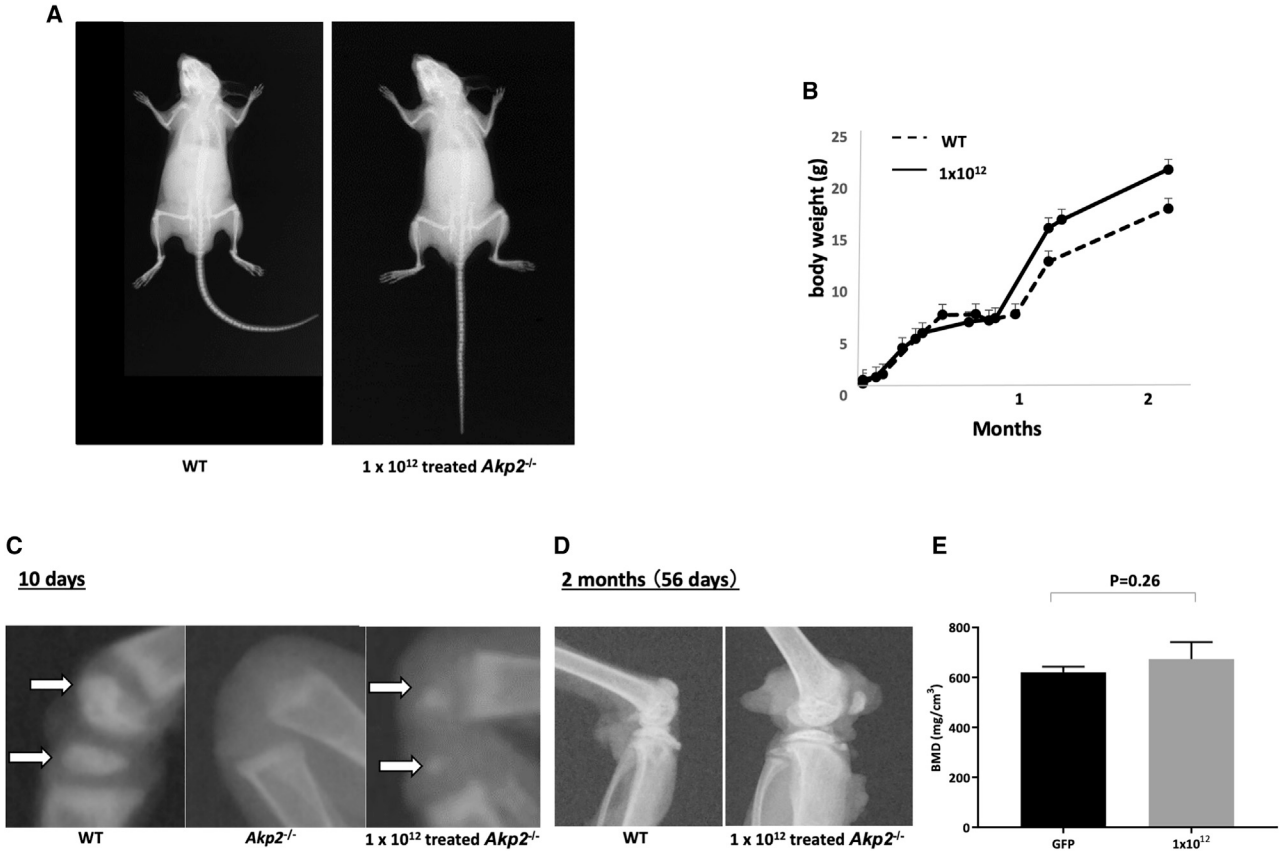

Figure 2. X-ray images and bone maturity of ARU-2801-treated *Akp2*$^{-/-}$ mice compared to WT mice, including body weight growth

(A) X-ray images at 2 months of age. Comparison of the posture and rough size of an *Akp2*$^{-/-}$ mouse treated with 1.0×10^{12} vg/body ARU-2801 and a WT mouse (at 100 mA, 40 kV for 30 s with μFX-1000 film). (B) Body weight development of WT (n = 3) and 1.0×10^{12} vg/body ARU-2801 (n = 5)-treated *Akp2*$^{-/-}$ mice at 2 months of age. (C) X-ray images of secondary ossification centers (arrow) on day 10 after birth. Secondary ossification centers were detected in all WT mice (left panel) but not in most *Akp2*$^{-/-}$ mice (middle panel). In contrast, secondary ossification centers were detected on day 10 after birth in 1.0×10^{12} vg/body ARU-2801-treated *Akp2*$^{-/-}$ mice (right panel). (D) X-ray analysis of knee joint at 2 months of age. X-ray images showed mature bone in 1.0×10^{12} vg/body ARU-2801-treated *Akp2*$^{-/-}$ mice (right panel) as being the same as in WT mice (left panel). (E) Bone mineral density (BMD) at 18 months of age. CT reconstruction of a femur in a 1.0×10^{12} vg/body ARU-2801-treated *Akp2*$^{-/-}$ (n = 3) and GFP-treated WT (n = 3) mice. Morphometric evaluation of cancellous bone. Data represent the mean ± SD.

versus 620.8 ± 52.9 mg/cm^3: p = 0.26) in the treated mice were not significantly different from those in the WT controls (Figure 2E).

ALP activity in the bones of mice treated with 1.0×10^{12} vg/body ARU-2801

Histological images of the knee joint are shown in Figure 3. ALP activity is revealed by fast blue staining. Blue-stained areas were seen in the surface of the endosteal bone and in the zone of resorption, where cartilage was calcifying in WT and 1.0×10^{12} vg/body ARU-2801-treated *Akp2*$^{-/-}$ mice.

Vector distribution shows restriction to injected muscle

Although the vector was injected intramuscularly, vector volume beyond the muscle's capacity may leak into the blood and circulate systemically. We previously reported that low AAV8-MCK-TNALP-D10 copy numbers were detected in the heart, liver, and bone following injections of 15 μL of AAV8-MCK-TNALP-D10 into the neonatal quadriceps femoris muscle.[18] Therefore, the distribution of 1.0×10^{12} vg/body ARU-2801 was analyzed in the liver, muscle, heart, and bone of treated mice. Using real-time PCR, we detected no AAV vector genome in any organ other than the ARU-2801-injected muscle. Since germline insertion of viral vector is important to assess for clinical use, we also analyzed the AAV vector genome in the testis and ovary of treated mice. ARU-2801 was not detected in the gonads and reproductive systems of treated animals. Real-time PCR revealed the presence of AAV vector only in muscle at the site of vector injection (data not shown).

No liver or kidney dysfunction was detected in treated *Akp2*$^{-/-}$ mice

In 1.0×10^{12} vg/body ARU-2801-treated *Akp2*$^{-/-}$ mice, biochemical data, liver and kidney function, and calcium levels were examined. Plasma calcium metabolism in all treated mice was similar to that in WT mice (calcium, 9.5 ± 0.45 versus 9.5 ± 0.63 mg/dL; p = 0.5). Liver

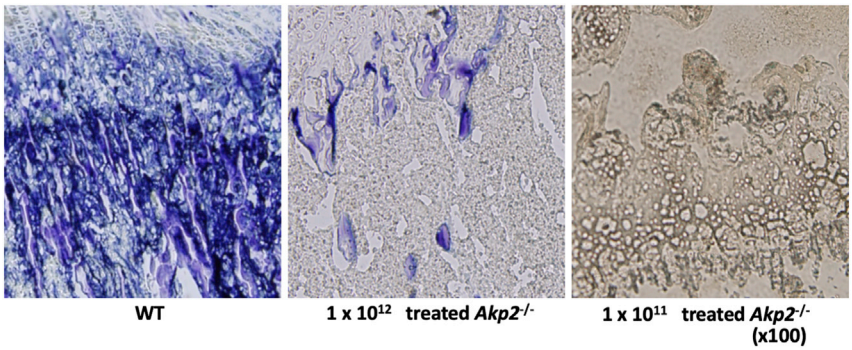

Figure 3. Histochemical staining of ALP activity in tibia

Fast blue staining of ALP activity in tibia at 2 months of age in WT mice and *Akp2*$^{-/-}$ mice treated with 1.0 × 10^{12} vg and 1.0 × 10^{11} vg of ARU-2801-vector. Original magnification, ×100.

and kidney function were in the normal range. Although the mice treated with 1.0 × 10^{12} vg/body ARU-2801 had plasma ALP activity (19.38 ± 5.02 U/mL) that was as much as 397-fold higher than endogenous levels in WT mice, there were no obvious problems in ARU-2801-treated mice. Furthermore, all organs looked normal macroscopically and no abnormal cell growth or tumors were observed.

Ectopic calcification seen on the paws of WT high-dose ARU-2801-treated mice with extremely high plasma ALP activity, but not with disease model ARU-2801-treated *Akp2*$^{-/-}$ mice

Constitutively high plasma ALP activity is not a physiological state. Therefore, to assess the safety and adverse effect of constitutively high plasma ALP activity, we injected large amounts of ARU-2801 into 6-week-old WT C57BL/6 mice. Mice injected with 5.5 × 10^{13} vg/body (n = 3), 55× the highest dose used in *Akp2*$^{-/-}$ mice, and followed until morbidity were seen around 6 months of age with high plasma ALP activity (8,347.3 ± 5,738.4 U/mL) (Figure 4A). All three mice administered this high-vector dosage developed calculi. One had a calculus in each metacarpal pad of the forepaw 2 months after injection and a small calculus in a digital pad of the left hind paw at 6 months. Another mouse had two calculi in each metacarpal pad at 2 months, while the third mouse had a small calculus in the digital pad of the left forepaw at 3 months. When mice (n = 3) were injected with a lower dose of vector (2.8 × 10^{13} vg/body, ∼28× the highest dose used in *Akp2*$^{-/-}$ mice), the level of ALP activity was about an order of magnitude less than with the 5.5 × 10^{13} vg/body dosage (373.0 ± 215.3 U/mL). In these mice, ectopic calcification started to appear about 4 months after injection. The calculi were solid and opaque to X-ray (Figure 4B). Infrared spectroscopy analysis of the stones by SRL (Tokyo, Japan) showed that they were composed mainly of calcium phosphate (55%) and calcium carbonate (45%). X-ray analysis revealed no calcification of blood vessels. Von Kossa staining showed no ectopic calcification in liver, heart, muscle, kidney, and blood vessels of these high-dose ARU-2801-treated WT mice. Additional WT C57BL/6 mice were also injected with lower doses of 1.1 × 10^{13} and 2.8x10^{12} vg/body (10× and ∼3× the highest dose used in *Akp2*$^{-/-}$ mice), and they showed no stones in their paws or any other surface of the body throughout the experiment period, i.e., 6 months. Importantly, note that in ARU-2801-treated *Akp2*$^{-/-}$ mice, no ectopic or vessel calcification (data not shown) was observed at the highest efficacious dose, i.e., 1.0 × 10^{12} vg/body.

DISCUSSION

We previously reported that intravenous AAV8 vector-associated systemic ERT achieved phenotype correction in *Akp2*$^{-/-}$ mice.[20] However, local intramuscular injection may prevent off-target effects, which have occurred with systemic AAV vector transfer.[21] Moreover, transduction to muscle cells with AAV vectors is likely to support sustained transgene expression because muscle cells are not dividing. AAV type 1-based intramuscular gene therapy is already certified to be safe for humans.[22] In the present study, we treated *Akp2*$^{-/-}$ mice with a single intramuscular injection of 1.0 × 10^{12} vg/body ARU-2801.

ARU-2801 was the same vector driven by the nonspecific constitutive promotor we used for intravenous systemic injection.[20] As with systemic administration, *Akp2*$^{-/-}$ mice treated with intramuscular injection exhibited high plasma ALP activity during 12 months (until sacrifice) and phenotypic correction. This result shows the efficacy of localized vector injection for treatment of *Akp2*$^{-/-}$ mice. Ideally, the AAV8 vector would remain in the muscle, producing enough TNALP to keep plasma ALP activity at a level sufficient to support bone mineralization, suppress seizures, and enable *Akp2*$^{-/-}$ mice to survive.

We previously observed that although the MCK promoter has the advantage of driving muscle-directed TNALP expression, the treated mice did not reach satisfactory bone maturity as compared to WT mice.[18,19] The promoter activity of tissue-specific promoter is weaker than that of tissue-nonspecific promoter. Moreover, tissue-nonspecific constitutive promoter has strong promoter activity in mammalian cells. We therefore aimed to achieve higher ALP expression and better bone maturation using an AAV vector encoding TNALP-D10 driven by the tissue-nonspecific constitutive promotor, which yielded high plasma ALP activity after systemic administration. To achieve sufficient plasma ALP activity with the MCK promoter, it was necessary to inject as much as 15 μL of vector into both quadriceps femoris muscles of neonatal mice (5.0 × 10^{12} vg/body). However, bone calcification still remained unsatisfactory. In the present study, in contrast, *Akp2*$^{-/-}$ mice lived healthily for 18 months, or nearly their entire lifetime, after a single intramuscular injection of only 2 μL of ARU-2801 administered during the neonatal period. The therapeutic effect of intramuscular injection was not inferior to that of systemic injection in terms of lifespan or physical phenotype. This suggests that the 2 μL of vector injected into the quadriceps femoris muscle of neonatal mice localized where it was injected. Muscular injection may be safer than intravenous injection because the vector

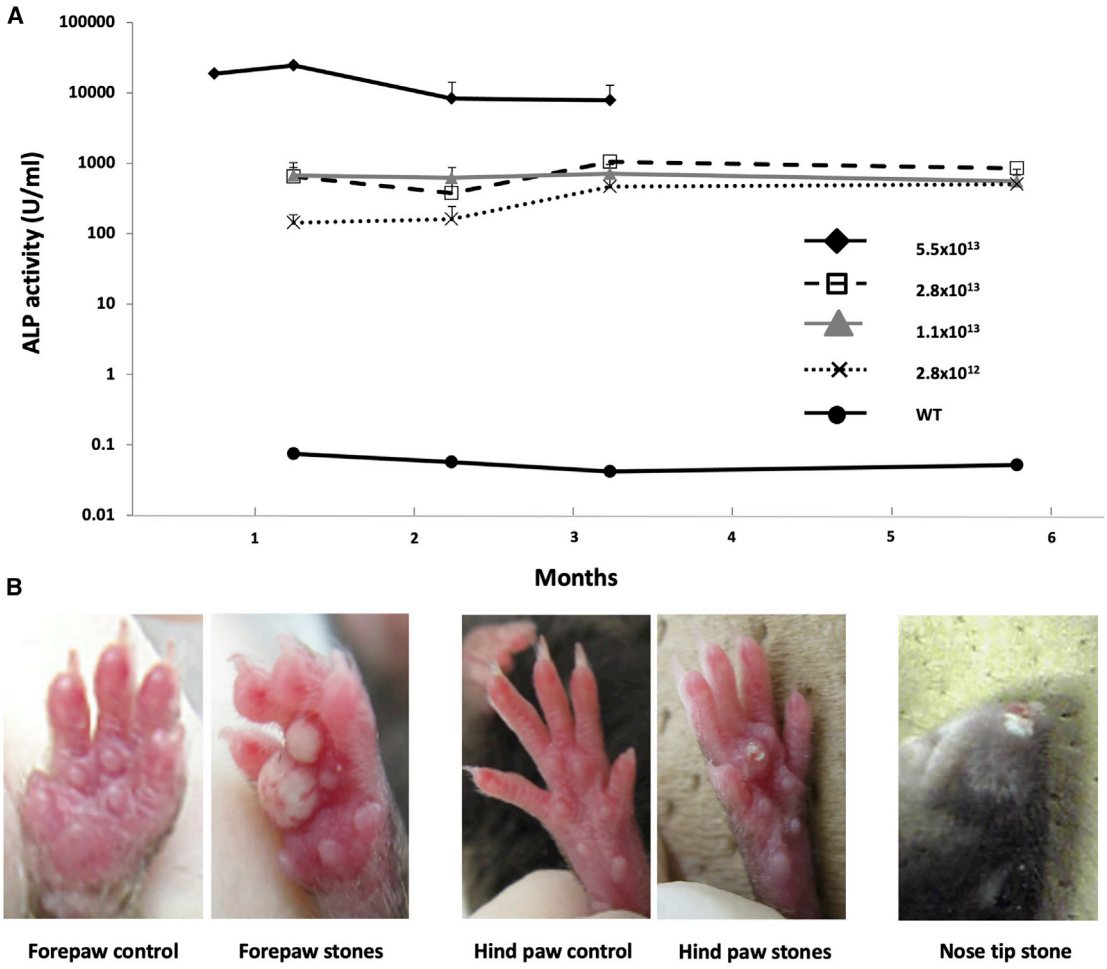

Figure 4. Calculi appeared on the paws of ARU-2801-injected C57BL/6 mice with extremely high plasma ALP activity

(A) Time-series plasma ALP activity after injection. ARU-2801 was injected into the right quadriceps femoris of 6-week-old male C57BL/6 mice at a dose of 2.8×10^{12}, 1.1×10^{13}, or 2.8×10^{13} vg/body in 50 μL of PBS, or at a dose of 5.5×10^{13} vg/body in 100 μL of PBS injected into both quadriceps (n = 3 in each group). (B) Shown are calculi in the forepaw and hind paw of 6-week-old C57BL/6 mice treated with 2.8×10^{13} (left panel) and 5.5×10^{13} (right panel) vg/body ARU-2801 vector. Note the presence of calculi at various sites.

stays in the muscle and is not distributed systemically. We also detected no liver or kidney dysfunction. Statistical analysis of CT data revealed increases in bone width and hyperplasia in the femurs of treated mice, and epiphysial cartilage structure was irregular. Diaphysis volume was nearly the same as in WT femurs. Given these results, it is our conjecture that the quality of the trabeculae in treated mice was nearly the same as in WT mice, although accelerated widening similar to flaring in rickets was found. Thus, a single intramuscular ARU-2801 injection during the neonatal period appears to be safe and effective for treatment of HPP.

The dose dependency of the response to systemic treatment for *Akp2*$^{-/-}$ mice was described previously.[20,23] It was therefore unexpected that after intramuscular injection of 3.0×10^{11} or 1.0×10^{12} vg/body ARU-2801, plasma ALP activity reached similar plateaus. Restricted to the muscle, the injected vector volume and thus TNALP expression likely reached an upper limit. If too large a vector volume was injected into the quadriceps, it would leak out of the muscle compartment and into circulation, effectively making the administration systemic. Consistent with that idea, we previously detected low AAV vector copy numbers in heart, liver, and bone after injection of 15 μL of AAV vector into the neonatal quadriceps femoris muscle.[18] By injecting only 2 μL of ARU-2801 in the present study, we limited the vector distribution to the muscle where it was injected; that is, there was no meaningful leakage of AAV8-TNALP-D10 from the muscle. Thus, although the constitutive promoter is not tissue specific, physical targeting to muscle was successfully achieved by injecting only a small volume of ARU-2801. This suggests that for clinical application of vector-related gene therapy, safer protocols may entail administration of smaller volumes capable of higher expression.

High-dose ARU-2801 injection led to unphysiologically high plasma ALP activity in 6-week-old WT C57BL/6 mice (~55× the dose used in *Akp2*$^{-/-}$ mice). Plasma ALP activity more than 1,000 U/mL after injection of 5.5 × 10^{13} vg/body vector into WT mice led to the emergence of soft tissue calcification within 2–3 months. WT mice injected with 2.8 × 10^{13} vg/body vector had lower plasma ALP levels, which delayed the soft tissue calcification, but calculi eventually developed after about 4 months. More investigation is needed to determine the threshold at which ALP activity begins to induce calcification of soft tissues. The reason why no calcification is found in other tissues except for the paw is unclear. It was reported that calcification in the paw is not very rare in animals because circulation is poor in pads due to its fiber-rich tissue, especially after trauma.[24] We speculate that the calcification in the paw can be occurred from poor circulation, gravity, and continuous irritation. Our preliminary experiments showed that extremely high ALP activity in WT mice (10,000 U/mL) causes ectopic calcification, regardless of the route of administration or the age of the mice at the time of administration (data not shown). The WT mouse with highest ALP activity suffered from calcification of the tip of its nose (Figure 4B, right panel), but an X-ray survey and Von Kossa staining showed no evidence of ectopic calcification elsewhere, such as the kidneys or blood vessels. Note that all calcification findings, however, were in high-dose-treated WT mice, and we did not observe calcification at any dose in *Akp2*$^{-/-}$ mice.

It has been reported that upregulation of TNALP plays an important role in medial vascular calcification.[25] Hyperphosphatemia is one of the symptoms associated with a disease state such as a malignant tumor or a metabolic bone disease such as osteomalasia, rickets, Paget disease, or osteoporosis, although a high plasma ALP level is not usually a cause of severe illness. Transient hyperphosphatasemia is sometimes seen in infants and during early childhood. These children exhibit plasma phosphatase levels that are about 5-fold higher than the normal range. This is usually referred to as "benign" hyperphosphatasemia. Nonetheless, among the young patients receiving ERT employing asfotase alfa, a bone-targeted recombinant human TNALP, none has experienced ectopic calcification or vascular calcification with plasma ALP activities as high as ~24 U/mL within 4 weeks of starting ERT[26] or 3–6 U/mL for 5 years after starting ERT therapy.[27] In the present study, we observed that plasma ALP activities of 5–10 U/mL after intramuscular ARU-2801 injection is sufficient for phenotypic correction of *Akp2*$^{-/-}$ mice. Although plasma ALP activities were up to 10-fold or more higher than the endogenous activity in untreated WT mice, no ectopic or aortic calcification was detected, nor were significantly abnormal calcium levels.[20] This suggests that while high plasma ALP activity may entail a risk of ectopic calcification, the clinically necessary ALP activity of around 5–10 U/mL appears safe and effective. The clinical application of ERT, asfotase alfa, was an important development for HPP patients,[28] while interruption meant sometimes death.[29] Frequent treatment for life could be a burden to the patients. We need to develop a new treatment with a simple method such as gene therapy.

In summary, we treated *Akp2*$^{-/-}$ mice with ARU-2801 gene therapy entailing a single intramuscular injection during the neonatal period. Treated mice exhibited high plasma ALP activity and lived for at least 18 months after injection, exhibiting normal function and behavior throughout their lives. This approach may be potentially safer than systemic administration, as there is no vector transfer to the brain or gonads and no oncogenic effects. This suggests AAV vector-related ERT may be a practical and useful approach to treating HPP patients.

MATERIALS AND METHODS

Cell culture

The HEK293 cell lines were cultured in Dulbecco's modified Eagle's medium (DMEM) supplemented with 10% fetal bovine serum, 50 U/mL penicillin and 50 μg/mL streptomycin under an atmosphere enriched with 5% CO_2.

Plasmid construction and vector production

To construct an AAV vector plasmid containing cDNA for expression of the human TNALP gene[30] with a constitutive promotor,[20] TNALP-D10 was prepared as described previously.[17] ARU-2801 was generated using the HEK293 cell line by the triple transfection method and purified as described previously.[31–33] Recombinant AAV8 vector encoding GFP (AAV8-GFP) was used as a control[34] for the evaluation of bone maturity at 18 months. AAV vector titers were determined using real-time PCR (7500 Fast, Applied Biosystems, Tokyo, Japan) as described previously.[31–33]

Enzyme activity and protein assay

ALP activity was determined as previously described.[35] One unit (U) was defined as the amount of enzyme needed to catalyze production of 1 μmol of *p*-nitrophenol per min. ALP activity in plasma was calculated as U/mL. ALP activity in organs was assayed in the supernatants of homogenized organs and standardized per mg of protein.[20]

Animal experiments

All animal experiments were performed using protocols approved by the Nippon Medical School Animal Ethics Committee. The generation and characterization of *Akp2*$^{-/-}$ mice were described previously.[36] To select *Akp2*$^{-/-}$ mice, all newborn TNALP/129/BL6 mice were genotyped using PCR as described previously.[20] The primers used were 5′-AGTCCGTGGGCATTGTGACTA-3′ and 5′-TGCTGCTCCACT CACGTCGAT-3′. The *Akp2*$^{-/-}$ mouse is a close phenotypic mimic of infantile HPP and has a healthy appearance when born. Growth retardation becomes apparent within the first week, and most *Akp2*$^{-/-}$ mice die within 2–3 weeks. About half of these mice have severe symptoms and experience epileptic seizures before death.[36] For this study, neonatal (1, 2 or 3 days after birth) *Akp2*$^{-/-}$ mice were injected with ARU-2801 (1.0 × 10^{11}, 3.0 × 10^{11}, or 1.0 × 10^{12} vg in 2 μL of PBS). We utilized TNALP/129/Bl6 *Akp2*$^{+/+}$ WT mice as controls for treatment experiment. WT mice were injected with AAV8-GFP vector (1.0 × 10^{12} vg/body in 2 μL of PBS) for 18 months of bone analysis as controls. The injections were made into the right quadriceps femoris muscle using a 22G Hamilton syringe (Osaka Chemical, Osaka, Japan). Blood samples were collected from the orbital sinus of anesthetized animals using heparin-coated capillaries, and plasma ALP activity was assessed at 1, 2, 3, 6, and 12 months (3.0 × 10^{11} vg/body in 2 μL

of PBS) and 1, 2, 3, 6, 12, and 18 months (1.0×10^{12} vg/body in 2 μL of PBS). The behavior of the mice was also observed. Mice were sacrificed under deep anesthesia by perfusion with PBS containing heparin (10 U/mL). Then, the organs of the mice were examined for macroscopic lesions. The organs were kept in a freezer at −80°C until analyzes.

To analyze the potential adverse effects of hyper-elevated plasma TNALP, 6-week-old male C57BL/6 mice purchased from Saitama Dobutsu Zikken were injected with a high dose of ARU-2801 (3.0×10^{12}, 5.5×10^{12}, 3.0×10^{13}, or 5.5×10^{13} vg/body in 50 μL of PBS) into the right quadriceps muscle using a 29G insulin syringe. The mice were then monitored for the appearance of ectopic calcification in their body, and analyzed for plasma ALP activity, plasma transaminase, and kidney function. Stones were analyzed at SRL (Tokyo, Japan).

X-ray analysis

X-ray analysis was performed as previously described.[20] In brief, radiographic images of adult mice were obtained on μFX-1000 film (Fujifilm, Tokyo, Japan) at an energy level of 25 kV and an exposure time of 10 s.

Biodistribution of AAV vector

The biodistribution of AAV vector was determined in *Akp2*$^{-/-}$ mice treated with ARU-2801. Genomic DNA was extracted from heart, liver, bone, and muscle and then subjected to real-time PCR as described previously.[20] The quadriceps from both legs were analyzed to compare the injected muscle with the contralateral untreated muscle.

Histological examination

To detect ALP activity, bone was directly stained without fixation or decalcification. Sections (10 μm thick) of the knee joints were cut using the Kawamoto film method.[20] ALP activity was assayed in the supernatant after biochemical tissue homogenization, and was histologically examined under a light microscope (BX60; Olympus, Tokyo, Japan) in tissues stained with fast blue. Von Kossa staining on liver, heart, muscle, kidney, and blood vessel sections were performed using a Von Kossa staining kit (ab150687, Abcam, Cambridge, MA, USA) according to manufacturer's instructions.

CT imaging and morphometric evaluation of cancellous bone

CT was carried out using a Latheta experimental animal CT system (LCT-200; Hitachi Healthcare, Tokyo, Japan) as described previously.[37] Bone morphometry was performed using Latheta software version 3.44 (Hitachi Healthcare) to determine bone mineral density (BMD). Continuous 48-μm slice images were utilized for quantitative assessments, and the cortical BMD was evaluated in 10 slices of the central part of the femur diaphysis.

Statistical analysis

Data from the experiments are expressed as means ± SD. Differences between groups were compared using Student's t test. p values less than 0.05 were considered statistically significant. Survival rates were analyzed using the Kaplan-Meier method, and differences in survival rates were assessed using the Wilcoxon test.

ACKNOWLEDGMENTS

We thank Dr. James Wilson at the University of Pennsylvania for providing AAV packaging plasmids (p5E18RXC1 and p5E18-VD2/8). We thank Prof. Norio Amizuka at Hokkaido University and Prof. Kimimitsu Oda at Niigata University for technical support with ALP activity staining. This study was supported by JSPS Grant-in-Aid for Scientific Research (KAKENHI) (C) grant no. JP 15K09605 and R01 DE12889 from the National Institute of Dental and Craniofacial Research (NIDCR), National Institutes of Health (NIH), USA, to J.L.M.

AUTHOR CONTRIBUTIONS

T.M., K.M., and T.S. conceived, designed, and administered the study, and all other authors assisted in its design. T.M., K.M., N.M., O.I., and K.A. performed experiments and analyzed data. O.I. and K.A. validated the experimental data. S.N. and J.L.M. provided the original HPP model *Akp*$^{-/-}$ mice. S.N., J.L.M., H.O., and T.S. made the original experimental methodology. T.M. wrote the manuscript with review comments from all authors. T.M. and K.M. edited the manuscript. All authors read and approved the final draft of the manuscript.

DECLARATION OF INTERESTS

The authors declare no competing interests.

REFERENCES

1. Mornet, E. (2007). Hypophosphatasia. Orphanet J. Rare Dis. *2*, 40.
2. Henthorn, P.S., and Whyte, M.P. (1992). Missense mutations of the tissue-nonspecific alkaline phosphatase gene in hypophosphatasia. Clin. Chem. *38*, 2501–2505.
3. Millán, J.L., and Whyte, M.P. (2016). Alkaline phosphatase and hypophosphatasia. Calcif. Tissue Int. *98*, 398–416.
4. Albeggiani, A., and Cataldo, F. (1982). Infantile hypophosphatasia diagnosed at 4 months and surviving at 2 years. Helv. Paediatr. Acta *37*, 49–58.
5. Whyte, M.P. (2016). Hypophosphatasia—Aetiology, nosology, pathogenesis, diagnosis and treatment. Nat. Rev. Endocrinol. *12*, 233–246.
6. Whyte, M.P., McAlister, W.H., Patton, L.S., Magill, H.L., Fallon, M.D., Lorentz, W.B., Jr., and Herrod, H.G. (1984). Enzyme replacement therapy for infantile hypophosphatasia attempted by intravenous infusions of alkaline phosphatase-rich Paget plasma: Results in three additional patients. J. Pediatr. *105*, 926–933.
7. Whyte, M.P., Magill, H.L., Fallon, M.D., and Herrod, H.G. (1986). Infantile hypophosphatasia: Normalization of circulating bone alkaline phosphatase activity followed by skeletal remineralization. Evidence for an intact structural gene for tissue nonspecific alkaline phosphatase. J. Pediatr. *108*, 82–88.
8. Weninger, M., Stinson, R.A., Plenk, H., Jr., Böck, P., and Pollak, A. (1989). Biochemical and morphological effects of human hepatic alkaline phosphatase in a neonate with hypophosphatasia. Acta Paediatr. Scand. Suppl. *360*, 154–160.
9. Camacho, P.M., Painter, S., and Kadanoff, R. (2008). Treatment of adult hypophosphatasia with teriparatide. Endocr. Pract. *14*, 204–208.
10. Whyte, M.P., Mumm, S., and Deal, C. (2007). Adult hypophosphatasia treated with teriparatide. J. Clin. Endocrinol. Metab. *92*, 1203–1208.
11. Whyte, M.P., Kurtzberg, J., McAlister, W.H., Mumm, S., Podgornik, M.N., Coburn, S.P., Ryan, L.M., Miller, C.R., Gottesman, G.S., Smith, A.K., et al. (2003). Marrow cell transplantation for infantile hypophosphatasia. J. Bone Miner. Res. *18*, 624–636.

12. Tadokoro, M., Kanai, R., Taketani, T., Uchio, Y., Yamaguchi, S., and Ohgushi, H. (2009). New bone formation by allogeneic mesenchymal stem cell transplantation in a patient with perinatal hypophosphatasia. J. Pediatr. *154*, 924–930.

13. Taketani, T., Oyama, C., Mihara, A., Tanabe, Y., Abe, M., Hirade, T., Yamamoto, S., Bo, R., Kanai, R., Tadenuma, T., et al. (2015). Ex vivo expanded allogeneic mesenchymal stem cells with bone marrow transplantation improved osteogenesis in infants with severe hypophosphatasia. Cell Transplant. *24*, 1931–1943.

14. Millán, J.L., Narisawa, S., Lemire, I., Loisel, T.P., Boileau, G., Leonard, P., Gramatikova, S., Terkeltaub, R., Camacho, N.P., McKee, M.D., et al. (2008). Enzyme replacement therapy for murine hypophosphatasia. J. Bone Miner. Res. *23*, 777–787.

15. Bowden, S.A., and Foster, B.L. (2018). Profile of asfotase alfa in the treatment of hypophosphatasia: Design, development, and place in therapy. Drug Des. Devel. Ther. *12*, 3147–3161.

16. Kishnani, P.S., Rush, E.T., Arundel, P., Bishop, N., Dahir, K., Fraser, W., Harmatz, P., Linglart, A., Munns, C.F., Nunes, M.E., et al. (2017). Monitoring guidance for patients with hypophosphatasia treated with asfotase alfa. Mol. Genet. Metab. *122*, 4–17.

17. Yamamoto, S., Orimo, H., Matsumoto, T., Iijima, O., Narisawa, S., Maeda, T., Millán, J.L., and Shimada, T. (2011). Prolonged survival and phenotypic correction of *Akp2*$^{-/-}$ hypophosphatasia mice by lentiviral gene therapy. J. Bone Miner. Res. *26*, 135–142.

18. Nakamura-Takahashi, A., Miyake, K., Watanabe, A., Hirai, Y., Iijima, O., Miyake, N., Adachi, K., Nitahara-Kasahara, Y., Kinoshita, H., Noguchi, T., et al. (2016). Treatment of hypophosphatasia by muscle-directed expression of bone-targeted alkaline phosphatase via self-complementary AAV8 vector. Mol. Ther. Methods Clin. Dev. *3*, 15059.

19. Ikeue, R., Nakamura-Takahashi, A., Nitahara-Kasahara, Y., Watanabe, A., Muramatsu, T., Sato, T., and Okada, T. (2018). Bone-targeted alkaline phosphatase treatment of mandibular bone and teeth in lethal hypophosphatasia via an scAAV8 vector. Mol. Ther. Methods Clin. Dev. *10*, 361–370.

20. Matsumoto, T., Miyake, K., Yamamoto, S., Orimo, H., Miyake, N., Odagaki, Y., Adachi, K., Iijima, O., Narisawa, S., Millán, J.L., et al. (2011). Rescue of severe infantile hypophosphatasia mice by AAV-mediated sustained expression of soluble alkaline phosphatase. Hum. Gene Ther. *22*, 1355–1364.

21. Donsante, A., Miller, D.G., Li, Y., Vogler, C., Brunt, E.M., Russell, D.W., and Sands, M.S. (2007). AAV vector integration sites in mouse hepatocellular carcinoma. Science *317*, 477.

22. Stroes, E.S., Nierman, M.C., Meulenberg, J.J., Franssen, R., Twisk, J., Henny, C.P., Maas, M.M., Zwinderman, A.H., Ross, C., Aronica, E., et al. (2008). Intramuscular administration of AAV1-lipoprotein lipase S447X lowers triglycerides in lipoprotein lipase-deficient patients. Arterioscler. Thromb. Vasc. Biol. *28*, 2303–2304.

23. Yadav, M.C., Lemire, I., Leonard, P., Boileau, G., Blond, L., Beliveau, M., Cory, E., Sah, R.L., Whyte, M.P., Crine, P., and Millán, J.L. (2011). Dose response of bone-targeted enzyme replacement for murine hypophosphatasia. Bone *49*, 250–256.

24. Tafti, A.K., Hanna, P., and Bourque, A.C. (2005). Calcinosis circumscripta in the dog: A retrospective pathological study. J. Vet. Med. A Physiol. Pathol. Clin. Med. *52*, 13–17.

25. Sheen, C.R., Kuss, P., Narisawa, S., Yadav, M.C., Nigro, J., Wang, W., Chhea, T.N., Sergienko, E.A., Kapoor, K., Jackson, M.R., et al. (2015). Pathophysiological role of vascular smooth muscle alkaline phosphatase in medial artery calcification. J. Bone Miner. Res. *30*, 824–836.

26. Kitaoka, T., Tajima, T., Nagasaki, K., Kikuchi, T., Yamamoto, K., Michigami, T., Okada, S., Fujiwara, I., Kokaji, M., Mochizuki, H., et al. (2017). Safety and efficacy of treatment with asfotase alfa in patients with hypophosphatasia: Results from a Japanese clinical trial. Clin. Endocrinol. (Oxf.) *87*, 10–19.

27. Whyte, M.P., Madson, K.L., Phillips, D., Reeves, A.L., McAlister, W.H., Yakimoski, A., Mack, K.E., Hamilton, K., Kagan, K., Fujita, K.P., et al. (2016). Asfotase alfa therapy for children with hypophosphatasia. JCI Insight *1*, e85971.

28. Hofmann, C.E., Harmatz, P., Vockley, J., Högler, W., Nakayama, H., Bishop, N., Martos-Moreno, G.Á., Moseley, S., Fujita, K.P., Liese, J., and Rockman-Greenberg, C.; ENB-010-10 Study Group (2019). Efficacy and safety of asfotase alfa in infants and young children with hypophosphatasia: A phase 2 open-label study. J. Clin. Endocrinol. Metab. *104*, 2735–2747.

29. Rockman-Greenberg, C. (2019). Letter to the Editor: "Efficacy and safety of asfotase alfa in infants and young children with hypophosphatasia: A phase 2 open-label study.". J. Clin. Endocrinol. Metab. *104*, 3146–3147.

30. Goseki-Sone, M., Orimo, H., Iimura, T., Miyazaki, H., Oda, K., Shibata, H., Yanagishita, M., Takagi, Y., Watanabe, H., Shimada, T., and Oida, S. (1998). Expression of the mutant (1735T-DEL) tissue-nonspecific alkaline phosphatase gene from hypophosphatasia patients. J. Bone Miner. Res. *13*, 1827–1834.

31. Salvetti, A., Orève, S., Chadeuf, G., Favre, D., Cherel, Y., Champion-Arnaud, P., David-Ameline, J., and Moullier, P. (1998). Factors influencing recombinant adeno-associated virus production. Hum. Gene Ther. *9*, 695–706.

32. Hermens, W.T., ter Brake, O., Dijkhuizen, P.A., Sonnemans, M.A., Grimm, D., Kleinschmidt, J.A., and Verhaagen, J. (1999). Purification of recombinant adeno-associated virus by iodixanol gradient ultracentrifugation allows rapid and reproducible preparation of vector stocks for gene transfer in the nervous system. Hum. Gene Ther. *10*, 1885–1891.

33. Kurai, T., Hisayasu, S., Kitagawa, R., Migita, M., Suzuki, H., Hirai, Y., and Shimada, T. (2007). AAV1 mediated co-expression of formylglycine-generating enzyme and arylsulfatase a efficiently corrects sulfatide storage in a mouse model of metachromatic leukodystrophy. Mol. Ther. *15*, 38–43.

34. Noro, T., Miyake, K., Suzuki-Miyake, N., Igarashi, T., Uchida, E., Misawa, T., Yamazaki, Y., and Shimada, T. (2004). Adeno-associated viral vector-mediated expression of endostatin inhibits tumor growth and metastasis in an orthotropic pancreatic cancer model in hamsters. Cancer Res. *64*, 7486–7490.

35. Sogabe, N., Oda, K., Nakamura, H., Orimo, H., Watanabe, H., Hosoi, T., and Goseki-Sone, M. (2008). Molecular effects of the tissue-nonspecific alkaline phosphatase gene polymorphism (787T > C) associated with bone mineral density. Biomed. Res. *29*, 213–219.

36. Narisawa, S., Fröhlander, N., and Millán, J.L. (1997). Inactivation of two mouse alkaline phosphatase genes and establishment of a model of infantile hypophosphatasia. Dev. Dyn. *208*, 432–446.

37. Okuda, T., Naruo, M., Iijima, O., Igarashi, T., Katsuyama, M., Maruyama, M., Akimoto, T., Ohno, Y., and Haseba, T. (2018). The contribution of alcohol dehydrogenase 3 to the development of alcoholic osteoporosis in mice. J. Nippon Med. Sch. *85*, 322–329.